JOURNAL OF RAMAN SPECTROSCOPY
J. Raman Spectrosc. 2001; **32**: 303–318

JRS

Conformational equilibria, Raman and infrared spectra and *ab initio* calculations of dichloromethylmethyldichlorosilane

V. Aleksa,[1†] A. Gruodis,[1†] D. L. Powell,[1‡] P. Klaeboe,[1*] C. J. Nielsen[1] and G. A. Guirgis[2§]

[1] Department of Chemistry, University of Oslo, P.O. Box 1033, N-0315 Oslo, Norway
[2] Department of Chemistry, University of Missouri–Kansas City, Kansas City, Missouri 64110-2499, USA

Received 16 February 2001; Accepted 24 February 2001

The infrared spectra of dichloromethylmethyldichlorosilane ($Cl_2CHCH_3SiCl_2$) were recorded in the vapour, amorphous and partly crystalline phases and when isolated in argon, nitrogen and krypton matrices at 5 K. Raman spectra of the liquid were recorded at various temperatures between 295 and 147 K. Spectra of the amorphous and annealed crystal deposited on a copper finger at 80 K were obtained. The spectra showed the existence of two conformers, *anti* and *gauche*, in the vapour and in the liquid. Approximately 12 infrared bands were reduced in intensity, and six of the same bands present in the fluid phases in the Raman spectra vanished upon crystallization. From the intensity variations of two band pairs with temperature, a $\Delta H°$ value of 0.4 ± 0.3 kJ mol^{-1} between the conformers was obtained in the liquid, *anti* being the low-energy conformer. Small increases and decreases in the IR band intensities were observed in the matrix spectra after annealing to 32 K (nitrogen), 36 K (argon) and 50 K (krypton). The enthalpy difference between the conformers is low in the matrices, but the *anti* conformer had lower energy than the *gauche* conformer. *Ab initio* calculations were performed at the HF/6–311G* level and gave optimized geometries, vibrational wavenumbers and infrared and Raman intensities for the *anti* and *gauche* conformers. The conformational energy derived was 4.4 kJ mol^{-1} with *anti* being the low-energy conformer. The dipole moments were calculated to be 1.2 and 3.1 D for the *anti* and *gauche* conformers, respectively. Correlation between the observed and calculated wavenumbers of both conformers revealed that *anti* was present in the crystal, and complete assignments of the spectra were carried out.

INTRODUCTION

Dichloromethylmethyldichlorosilane ($Cl_2CHCH_3SiCl_2$) (DCMDCS) was synthesized and a vibrational spectroscopic study was carried out. The complete results of this investigation are described in this paper; a preliminary communication was published earlier.[1] The molecule can exist in two conformations, *anti* and *gauche*, as shown in Fig. 1. The infrared and Raman spectra of DCMDCS were investigated among a series of halogenated silanes, the results of which have recently been reported. Various silanes with conformational equilibria containing one silicon atom have been studied,[2–7] and molecules with two[8–13] and three[14–16] silicon atoms have recently been investigated by Hassler and co-workers[8–16] and their vibrational spectra reported, combined with studies by gaseous electron diffraction.[12]

The interactions between the end groups around a C—Si bond are smaller than in the corresponding ethanes with a C—C bond. This is confirmed by results of quantum chemical calculations and experiments, which show that most of the fundamentals of the *anti* conformer overlap with those of the *gauche* conformer in silanes with a central C—Si bond. The calculations on DCMDCS suggested that 19 of the 27 vibrational modes of the *anti* and *gauche* conformers were separated by less than 10 cm^{-1}. The IR bands recorded in inert matrices, however, are very sharp, frequently making a distinction between close neighbour bands of the two conformers feasible.

*Correspondence to: P. Klaeboe, Department of Chemistry, University of Oslo, P.O. Box 1033, N-0315 Oslo, Norway.
Email: peter.klaboe@kjemi.uio.no
†Permanent address: Department of General Physics and Spectroscopy, Vilnius University, Vilnius 2734, Lithuania.
‡Permanent address: Department of Chemistry, College of Wooster, Wooster, Ohio 44691, USA.
§Permanent address: Bayer Corp., Bushy Park Plant, Research and Development, Charleston, South Carolina 29423-8088, USA.

DOI: 10.1002/jrs.702

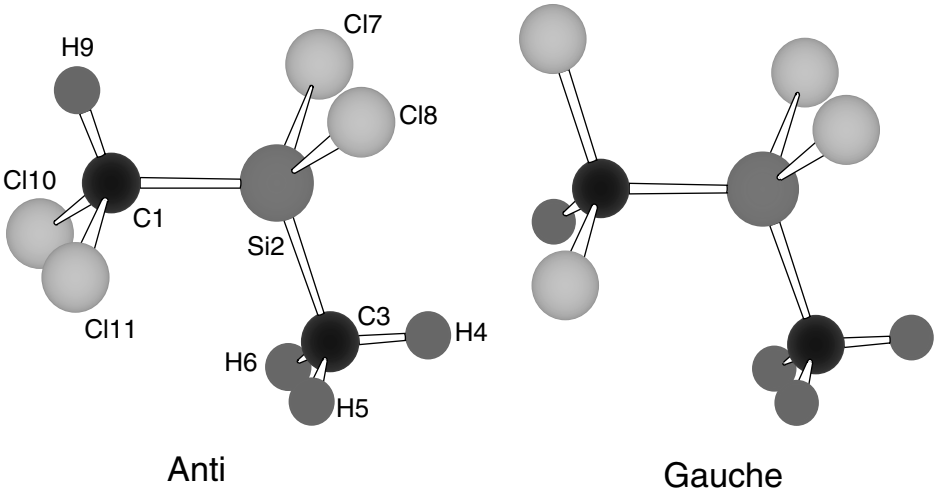

Figure 1. The *anti* and *gauche* conformers of dichloromethylmethyldichlorosilane (DCMDCS) including numbering of atoms for the definition of symmetry coordinates.

EXPERIMENTAL

Sample preparation

The compound was prepared by the chlorination of dimethyldichlorosilane in the presence of carbon tetrachloride in the vapour phase.[17] A mixture of DCMDCS and chloromethylmethyldichlorosilane was formed and separated by fractional distillation. The product was purified in a low-temperature, low-pressure fractionation column and the purity was checked by mass spectrometry. The IR vapour spectra revealed an impurity of hydrogen chloride, which was reduced by pumping off the HCl at ~220 K on a vacuum line.

Raman spectral measurements

Raman spectra were recorded with a triple monochromator spectrometer from Dilor (Model RTI-30), using 514.5 nm radiation from a Spectra-Physics Model 2000 argon ion laser for excitation. A capillary of 2 mm i.d. was employed. Raman spectra of the liquid in two directions of polarization were recorded at room temperature. Additional spectra were obtained at 10 different temperatures between 295 and 147 K in a capillary tube of 2 mm i.d. surrounded by a Dewar vessel, cooled by gaseous nitrogen evaporated from a reservoir.[18] DCMDCS forms a supercooled liquid which spontaneously crystallized, as observed for a series of other halogenated silanes. From the variable-temperature spectra the enthalpy difference ΔH in the liquid between the conformers was calculated. Low-temperature spectra were also obtained on a copper finger, cooled by liquid nitrogen. Almost complete crystallization was obtained in the Raman cryostat after annealing to 150 K.

Infrared spectral measurements

The infrared spectra were recorded on various Fourier transform spectrometers in the mid-infrared (MIR) region: Bruker IFS-88 (4000–450 cm^{-1}) and IFS-66 (4000–450 cm^{-1}), spectrometers and a Perkin-Elmer Model 2000 (4000–450 cm^{-1}). A Bruker Model IFS-113v vacuum spectrometer was employed in the far-infrared (FIR) region (600–50 cm^{-1}). All these instruments had DTGS detectors, and beamsplitters of Ge substrate on KBr were employed in the MIR, whereas Mylar beamsplitters of 3.5, 6.25 and 12 μm thickness and a beamsplitter of metal mesh were used in the FIR region.

The vapour spectra were recorded in a folded cell, adjusted to ~3 m pathlength (KBr windows), a cell of 10 cm pathlength (CsI windows) in MIR and a cell with 20 cm pathlength (PE windows) in FIR. The sample was studied in an MIR cryostat with inner and outer windows of CsI, and in an FIR cryostat with an inner window of wedge-shaped silicon and outer windows of PE, both cooled with liquid nitrogen.

The sample was diluted with argon, nitrogen and krypton (1 : 1000) and deposited on a CsI window at 5 K of a closed cycle He-cooled cryostat from APD (Model HS-4) with a three-stage cooling system. The spectra of the unannealed matrices were first recorded. Subsequently, the matrices were annealed to temperatures between 15 and 20 K to remove site effects in the matrices, then they were annealed in steps of 3–5 K to a maximum of 36 K in argon, 32 K in nitrogen and 50 K in krypton, in periods of annealing time from 10 min to 1 h. Higher temperatures cannot be employed since the inert gases have too high a pressure in the cryostat and also the matrices turn 'soft' followed by diffusion of the solute.[19] After each annealing the window was recooled to 5 K and the spectra were recorded.

RESULTS

Raman spectral results

Raman spectra of DCMDCS as a liquid in two directions of polarization in the range 3020–2880 and 900–50 cm^{-1} are

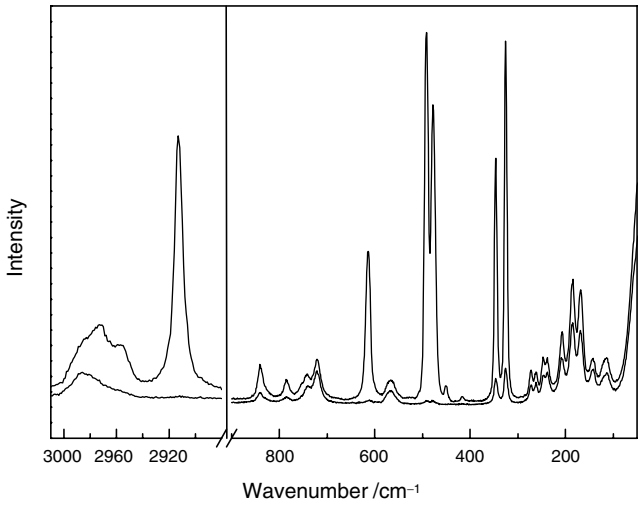

Figure 2. Raman spectra of DCMDCS as a liquid in two directions of polarization in the regions 3020–2880 and 900–50 cm^{-1}.

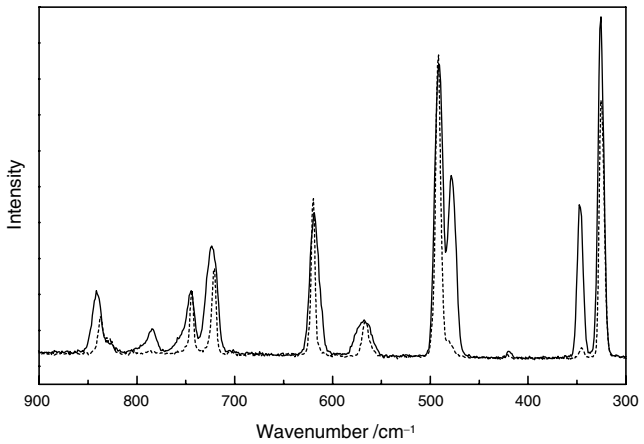

Figure 3. Raman spectra of DCMDCS in the range 900–300 cm^{-1} as an amorphous sample (solid line) and as a crystalline solid, annealed to 150 K (dashed line) recorded at 80 K.

given in Fig. 2; the very weak fundamentals in the range 1500–900 and the combination bands between 2880 and 1500 cm^{-1} are not shown. The vapour was condensed on a finger of copper kept at ~80 K in a Raman cryostat, cooled by liquid nitrogen. The solid deposit appeared glassy and the Raman spectrum was similar to that of the liquid. This deposit was annealed in order to facilitate crystallization, and eventual changes were observed both visually when the solid changed from a glassy to a frosty look and from inspection of the recorded spectra. In the temperature region around 150 K, the deposit changed appearance and a predominantly crystalline solid was formed. The Raman spectrum of the crystal had sharper bands, frequently shifted from the position in the amorphous phase. Also, lattice modes were observed in the low-wavenumber region at 47, 37 and 31 cm^{-1}. Raman spectra of the amorphous and crystalline solids, both recorded at 80 K, are given in Fig. 3 (900–300 cm^{-1}); corresponding spectra in the range 550–300 and 300–50 cm^{-1} have been presented earlier.[1] The experimental results obtained from the Raman and infrared spectra are listed in Table 1. The most intense Raman band is found at 491 cm^{-1} in the liquid and is connected with symmetric $SiCl_2$ stretch, while the symmetric CCl_2 stretch at 614 cm^{-1} has a lower intensity.

As is apparent from Fig. 3 and the data in Table 1, the six Raman bands situated at 1266, 787, 478, 347, 246 and 122 cm^{-1} in the liquid vanish after crystallization. They are assigned to the conformer which is not present in the crystal. This conformer also has a higher energy in the liquid and probably in the vapour phase, and shown below this is the *gauche* rotamer, whereas the *anti* conformer is present in the crystal.

Raman spectra of the liquid were recorded at 10 temperatures in the range between 295 and 147 K. Only small intensity variations of certain bands relative to neighbouring bands with changing temperature were observed in the spectra of the liquid, interpreted as a displacement of the conformational equilibrium. Among the number of *anti–gauche* band pairs observed, the Raman pairs 326/347, 491/478 and 262/272 cm^{-1} were tested. The bands in the nominator were present (*anti*) and those of the denominator (*gauche*) vanished in the crystal. It was found that the band pair 262/272 cm^{-1} gave values deviating from those of the other band pairs. This is not unexpected since the 272 cm^{-1} band did not vanish completely in Raman spectra of the crystal, but a very weak peak remained at 268 cm^{-1}, possibly due to a contribution from an overtone or combination band of the other conformer. Moreover, the bands 262/272 cm^{-1} were weak whereas those of the two other band pairs were all strong or very strong.

The intensities of each band pair were fitted to the equation $\ln K = -\Delta H/RT + \text{constant}$, where K is the ratio of peak heights or integrated areas I_{anti}/I_{gauche}, and it is assumed that ΔH is constant with temperature. The van't Hoff plots based upon measured peak heights (PH) and integrated areas (IA) have been presented earlier.[1] They gave the values for $\Delta H(gauche - anti)$ of 0.31, 0.39 (PH) and 0.42, 0.58 (IA) kJ mol^{-1} based upon the pairs 491/478 and 326/347 cm^{-1}, respectively. The average value $\Delta H(gauche - anti)$ was 0.4 ± 0.3 kJ mol^{-1}. In corresponding measurements on other silanes[20–27] it was found that the peak heights generally gave more reliable values, with smaller standard deviations, than integrated areas.

Infrared spectral results

MIR vapour spectra of DCMDCS in the region 1450–500 cm^{-1} recorded at pressures of ca 2 and 0.5 Torr (1 torr = 133.3 Pa) in a folded vapour cell with ca 3 m pathlength is presented in Fig. 4. Owing to the large moments of inertia caused by the four chlorine atoms, very few vapour contours are resolved.

Table 1. Infrared and Raman spectral data[a] for dichloromethylmethyldichlorosilane (DCMDCS)

Infrared						Raman				
				Solid			Solid			
Vapour 298 K[b] $\tilde{\nu}$/cm^{-1}	Ar matrix 5 K[b] 20–38 K[c] $\tilde{\nu}$/cm^{-1}	N_2 matrix 5 K[b] 20–33 K[c] $\tilde{\nu}$/cm^{-1}	Kr matrix 5 K[b] 20–50 K[c] $\tilde{\nu}$/cm^{-1}	Annealed 80 K[b] 135 K[c] $\tilde{\nu}$/cm^{-1}	Crystal 80 K[b] 150 K[c] $\tilde{\nu}$/cm^{-1}	Liquid 295 K[b] $\tilde{\nu}$/cm^{-1}	Amorphous 80 K[b] $\tilde{\nu}$/cm^{-1}	Crystal 80 K[b] 150 K[c] $\tilde{\nu}$/cm^{-1}	Conformer *anti*	Conformer *gauche*
2987 w	2999 vw			2988 m	2987 vw	2989 m, D		2991 m	ν_2	ν_2
						2983 w, P		2983 m		
2965 w	2970 vw			2973 s	2973 s	2975 m, P	2979 m	2978 m	ν_1	ν_1
2952 vw	2952 vw			2957 m	2958 m	2957 m, P			ν_3	ν_3
2919 w				2911 m	2915 vw 2909 w	2916 vs, P	2915 s	2914 s	ν_4	ν_4
	2887 m/w									
	2885 w		2873 vw↓							
2851 vw				2850 vw	2850 vw	2833 vvw				
							1413 vw			
1414 w	1410 w			1413 s	1413 s	1406 vw, P?	1407 vw	1407 vw	ν_5	ν_5
	1407 w			1406 w	*					
1408 w	1405 w	1405 w	1403 w	1399 s	1393 s	1398 vvw	1404 vw	1404 vw	ν_6	ν_6
							1402 vw	1398 vw		
				1368 w	1368 w		1393 vw			
				1348 w	1347 w					
1272 m										
1270 m			1271 s ↓ 1269 s ↑	1264 vs	*	1266 vw, P	1265 vw	*		ν_7
1267 s	1262 s↑	1265 s↑	1261 s↑	1259 vs	1259 vs 1257 s	1260 vw	1260 vw	1260 vw	ν_7	
1262 m										
1260 w										
			1202 vw							
1191 w	1194 w ↓ 1189 vw ↓	1198 w	1190 vw	1192 m	*					ν_8
	1185 w↑	1199 vw	1187 w↑	1188 m	1188 m	1193 w, P?	1192 w	1195 w	ν_8	

JRS

1146 m 1141 m	1133 w↑	1150 w	1142 vw 1137 vw	1141 m		1144 w, P?	1143 w	1142 vvw	ν_9	ν_9
1094 m, br		1094 w		1093 m						
848 w	839 w 837 m ↓	845 m 842 m	842 w 839 w ↓							ν_{10}
841 m	836 m ↑ 835 w	837 m↑	836 m 834 w ↑	838 s	837 m	839 w, P	837 w	837 w	ν_{10}	
826 w	826 w 824 w	825 w		825 w	825 w	828 vw, D?	826 vw	827 vw	ν_{11}	ν_{11}
798 s 796 s	798 m ↑ 796 s 795 s 792 s ↑	799 m ↑ 797 vs 795 s 792 s ↑	795 vs	795 s	794 s	800 vw	794 vw		ν_{12}	
791 m	788 s ↑ 785 s ↑	789 s 788 s 786 s ↑	785 vs	788 s	784 w(*)	787 m, P	785 m	*		ν_{12}
745 s	748 w	747 m↓	744 w↓	756 m	756 vw(*)					ν_{13}
741 s	742 m↑	743 s↑	742 w↑	749 m 743 s	749 w 740 s	741 w, P	745 w	744 w	ν_{13}	
	735 w	739 vw	740 m↑ 736 vw							
732 s	728 w↓	731 m ↑ 729m ↑	733 w↑	727 s	724 vw(*)					ν_{14}
728 m	726 w ↓ 723 m ↑ 722 m ↑ 720 w↑	726 m 724 m ↑ 721 m ↑	725 m 723 m ↑ 722 m ↑ 720 m↑	720 s	719 s	721 m, D	722 m	721 m	ν_{14}	
	623 w									
	620 m↑	621 m↓	622 m							
615 m	617 m↑	617 m↑	618 m	620 m	622 s	614 s, P	619 m	620 m		ν_{15}
	614 w↑	613 m	615 m	616 m	610 vw(*)				ν_{15}	

(*continued overlead*)

Infrared						Raman				
				Solid			Solid			
Vapour 298 K[b] $\tilde{\nu}$/cm^{-1}	Ar matrix 5 K[b] 20–38 K[c] $\tilde{\nu}$/cm^{-1}	N_2 matrix 5 K[b] 20–33 K[c] $\tilde{\nu}$/cm^{-1}	Kr matrix 5 K[b] 20–50 K[c] $\tilde{\nu}$/cm^{-1}	Annealed 80 K[b] 135 K[c] $\tilde{\nu}$/cm^{-1}	Crystal 80 K[b] 150 K[c] $\tilde{\nu}$/cm^{-1}	Liquid 295 K[b] $\tilde{\nu}$/cm^{-1}	Amorphous 80 K[b] $\tilde{\nu}$/cm^{-1}	Crystal 80 K[b] 150 K[c] $\tilde{\nu}$/cm^{-1}	Conformer	
									anti	*gauche*
580 vs	576 vs ↓ 575 vs ↑ 574 vs 573 m ↑	574 vs	574 vs 573 vs ↑ 571 vs 570 s ↑	574 s	572 s	566 vw, br, D	568 vw, br	566 vw, br	ν_{16}	
575 vs	571 m ↓ 570 m ↑	571 m	569 s ↓ 567 m ↓ 565 m 563 w	565 s	561 vw(∗)		563 vw			ν_{16}
500 m, sh		499 w↑								
498 m 494 m, Q 490 m	494 m 491 m	493 vs ↓ 491 s ↑	494 m ↑ 492 m ↑	492 s	489 s	491 vs, P	491 vs	492 vs	ν_{17}	
	488 w		489 m 479 w							
478 m	481 w	481 w 472 w↑	478 w 475 w	477 m	481 w(∗)	478 s, P	478 s	∗		ν_{17}
				449 vw	450 vw	450 m, P				
346 w				346 s	348 vw(∗) 344 vw(∗)	347 vs, P	347 m	∗		ν_{18}
327 w 325 w, Q 323 w				325 m 322 w	325 m 322 m	326 vs, P	326 vs	325 vs	ν_{18}	
266 w, sh				272 w	273 vw(∗)	272 w, P	274 w	268 vw(∗)		ν_{19}
261 m				262 w	263 w 259 m	262 w, D?	261 w	258 w	ν_{19}	
248 vw				246 w	246 vw(∗)	246 m, P	243 w	∗		ν_{20}

JRS

239 vw	236 w	240 w	238 m, P?	237 m	241 m	ν_{20}	
206 w, sh							
204 w	206 s	208 s, 206 s	206 m, P	205 m	208 m	ν_{21}	ν_{21}
194 vw	189 vw	187 w	185 s, P?	187 m	194 m	ν_{22}	ν_{22}
				185 m	185 vw		
172 vw	170 w	168 w	169 s, P?	174 m, sh	176 m	ν_{23}	ν_{23}
			165 w	167 m	165 m		ν_{24}
			155 w	156 w	153 w	ν_{24}	
	148 w, br	145 m	148 w, D	146 w	150 w	ν_{25}	
	140 w	*	122 vw	123 w	*		ν_{25}
	114 w, br	112 w	115 w, P	115 vw	111 vw		ν_{26}
			111 vw, D	76 m	*	ν_{26}	
	72 w	73 w	62 vw	67 m	59 s	ν_{27}	ν_{27}
					47 m		
					37 s		
					31 w		

[a] Abbreviation: s, strong; m, medium; w, weak; v, very; sh, shoulder; bd, broad; P, polarized; D, depolarized; asterisks denote bands vanishing in the crystal spectra; asterisks in parentheses mean bands being reduced in intensity in the crystal; arrows pointing upwards and downwards signify bands which increase and decrease in intensity, respectively, after annealing.

[b] Recording temperature.

[c] Annealing temperature.

JRS

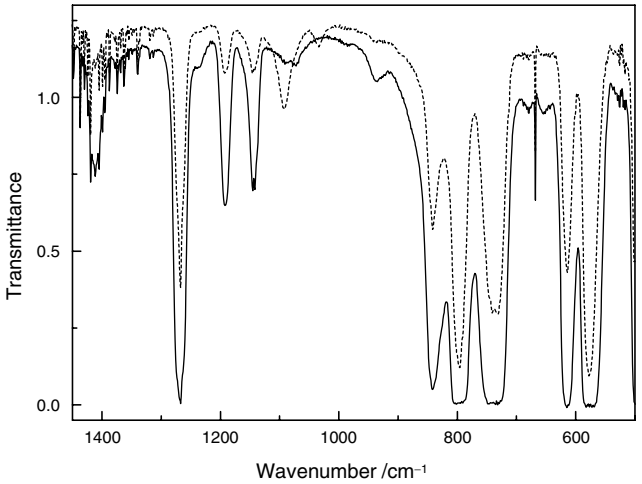

Figure 4. MIR spectra of DCMDCS as a vapour at ~2 Torr (solid line) and 0.5 Torr pressures (dashed line) in the range 1450–500 cm^{-1} in a folded cell of ca 3 m pathlength.

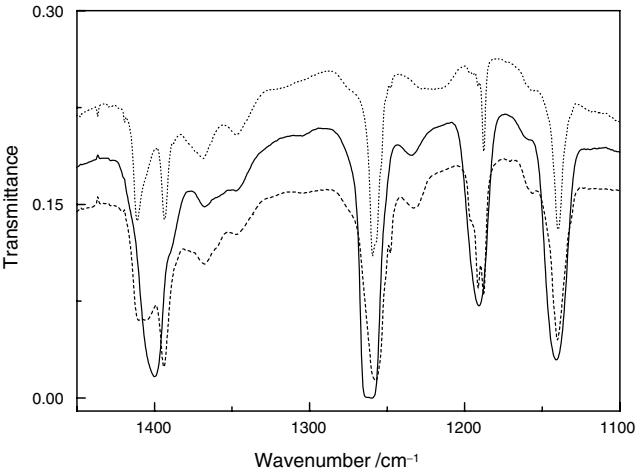

Figure 5. MIR spectra (1450–1100 cm^{-1}) of DCMDCS as unannealed solid (solid line), annealed to 135 K (dashed line) and to 150 K (dotted line), recorded at 80 K.

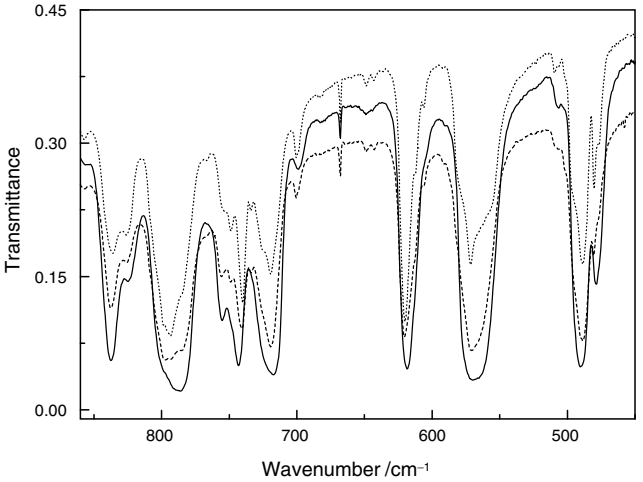

Figure 6. MIR spectra (860–450 cm^{-1}) of DCMDCS as unannealed solid (solid line), annealed to 135 K (dashed line) and to 150 K (dotted line), recorded at 80 K.

Also, it is difficult to decide if the apparent band structure is a result of resolved rotational contours or is due to overlapping fundamentals from the two conformers. The most intense IR band, found at 580 cm^{-1}, is attributed to $SiCl_2$ asymmetric stretch.

The vapour was condensed on a CsI window at 80 K and various spectra were recorded in which the sample was annealed and recooled to 80 K, but in other series the spectra were recorded at the annealing temperature. A large number of annealing experiments were carried out in the infrared cryostats since crystallization was much more difficult to achieve than in the corresponding Raman experiments.

An amorphous phase was formed when the vapour was deposited on the CsI (MIR region) or the silicon window (FIR region) at 80 K. It has frequently been experienced that the thin layer of sample employed in the infrared cryostats makes crystallization difficult to achieve. On the other hand, the larger sample concentrated on a small area of the copper finger in the Raman cryostat may form crystals readily. This was the case in DCMDCS and, in spite of much effort, only partial crystallization was achieved in the infrared cryostats, as the bands expected to vanish were merely reduced in intensity.

It was observed that annealing to an intermediate temperature of 135 K was followed by a change in the appearance and the sample looked crystalline from visual observation. Moreover, the bands became sharper and were frequently shifted from those of the amorphous, unannealed sample. However, none of the bands which vanished in the Raman spectra after annealing: 1264, 788, 477, 349/346, 246 or 140 cm^{-1} disappeared in this phase. It is possible that this solid phase was a plastic crystal.

When the sample was annealed to ca 150 K (the temperature which was employed to obtain the crystalline phase in the Raman cryostat), further changes occurred in the IR spectrum and some bands partly disappeared. Apparently, a mixture of amorphous, intermediate and crystalline solids is present in the MIR and FIR spectra observed. These spectra are presented with reasonably high dispersion in Figs 5 (1450–1100), 6 (860–450) and 7 (520–100 cm^{-1}) in order to make the spectral changes visible. As is apparent, the IR bands at 1264 and 1192 cm^{-1} of the intermediate phase annealed to 135 K disappeared completely after annealing to 150 K, whereas those at 788, 756, 727, 565, 477, 346, 272 and 140 cm^{-1} vanished partially. Some of these bands (756, 727, 616 and 565 cm^{-1}) were not detected in the Raman spectra. Splitting into doublets of certain IR bands remaining in the spectra after annealing to 150 K was observed at 2915/2909, 1259/1257, 749/740, 325/322, 263/259 and 208/206 cm^{-1} and reveal at

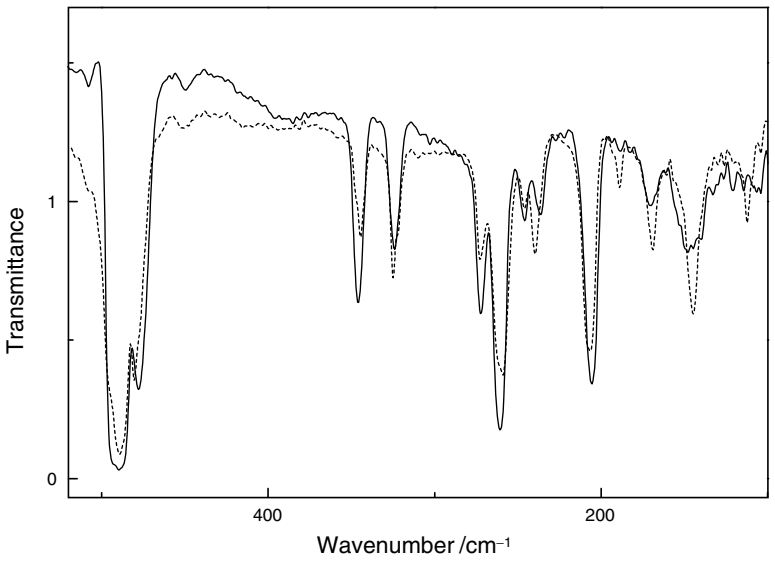

Figure 7. FIR spectra (520–100 cm^{-1}) of DCMDCS as unnannealed solid (solid line) and annealed to 150 K (dashed line) recorded at 80 K.

least partial crystallinity of the solid containing the *anti* conformer.

The sample was mixed with argon, nitrogen and krypton in 1 : 1000 ratios and deposited at 5 K. As it is frequently observed that matrix isolated spectra can vary considerable with the matrix gas employed, three different matrix gases were used. The annealing temperatures which can be employed are restricted by the vapour pressure and the rigidity of the matrices.[19] Infrared spectra of the matrices were recorded before annealing and after annealing at 24, 26, 29, 32 and 34, 36 and 38 K in argon and at 25, 31 and 33 K in nitrogen matrices. Krypton matrices have lower vapour pressure and can therefore be annealed to higher temperatures. These spectra were recorded after annealing to 20, 25, 30, 35, 40, 45 and 50 K. After a ca 15 min annealing time the sample was recooled to 5 K before the spectra were recorded.

Detailed infrared matrix spectra before and after annealing are presented in Figs 8 (argon, 870–700 cm^{-1}) and 9 (krypton, 1280–1250 and 585–550 cm^{-1}). Previously, the IR spectra in nitrogen matrices have been presented[1] in the region 810–710 cm^{-1}. The bands of the matrix spectra are very sharp, frequently giving separate peaks for the two conformers which overlap in the vapour and in the condensed phases. Supposedly, the conformational equilibrium of the vapour phase is maintained when the gas mixture hits the CsI window at ca 5 K unless the barrier is extremely low. The high-energy conformer may pass the potential barrier and convert to that of low energy when the temperature is raised. Only small spectral changes occurred in all the matrices when the samples were annealed, suggesting either a high barrier or a small enthalpy difference between the conformers in the matrices.

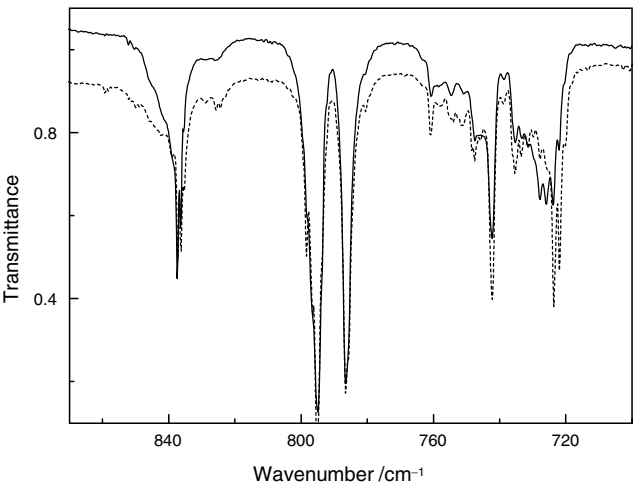

Figure 8. MIR spectra of DCDMDCS in the range 870–700 cm^{-1} in an argon matrix (1 : 1000) deposited and recorded at 5 K: unannealed sample (solid line) and sample annealed to 34 K (dashed line).

It was observed that in most cases the IR bands present in the crystal were enhanced and those absent in the crystal diminished in intensity after the matrices were annealed to temperatures above ca 34 K, but some cases were uncertain. The bands which are enhanced or reduced in intensity after annealing are marked with arrows pointing upwards or downwards, respectively, in Table 1. From the plots given by Barnes,[28] the barrier height should be around 8 kJ mol^{-1}. Secondary effects due to matrix viscosity or matrix–solute interactions might influence the barrier height, but supposedly the value also applies to the isolated molecules in the vapour phase.

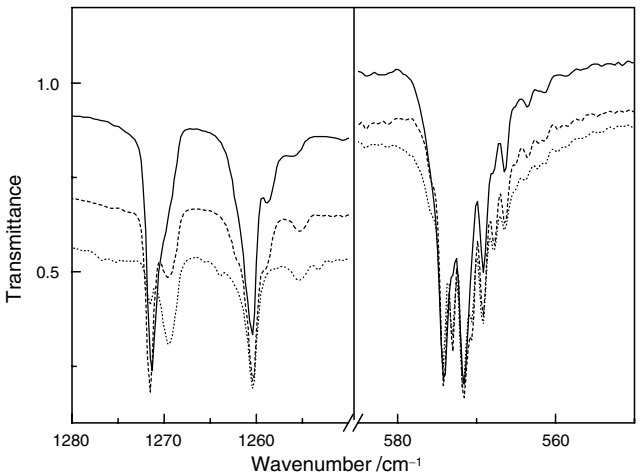

Figure 9. MIR spectra of DCDMDCS in the range 1280–1250 and 585–550 cm^{-1} in a krypton matrix (1 : 1000) deposited and recorded at 5 K: unannealed sample (solid line) and sample annealed to 36 K (dashed line) and to 45 K (dotted line).

Quantum chemical calculations

Hartree–Fock (HF) quantum chemical calculations were performed using the Gaussian 94 program.[29] To allow an easy comparison with the series of halomethyldimethylhalosilanes studied,[20–27] the 6–311G* basis set was employed for the whole series. The minima on the potential surface were found by relaxing the geometry; the bond distances and angles for the *anti* and *gauche* conformers have not been presented for the sake of brevity.

The conformational energy difference was calculated to be 4.4 kJ mol^{-1} with *anti* being the low-energy conformer, much larger than the experimental results of the liquid ΔH $(gauche - anti) = 0.4 \pm 0.3$ kJ mol^{-1}.

Normal coordinate calculations

Analytical Hartree–Foch force constants were calculated for each of the two conformers of DCMDCS. The *ab initio* force constants were transformed from Cartesian to symmetry coordinates, derived from a set of valence coordinates. The *ab initio*-calculated wavenumbers are invariably larger than the experimental values. In order to make a complete assignment of the observed infrared and Raman bands, a normal coordinate analysis with scaled force constants was carried out. Scaling factors of 0.9 for the stretching and bending modes above and no scaling for the modes below 400 cm^{-1} were employed in accordance with the procedure applied to the related silanes.[20–27] The infrared intensities, Raman scattering cross-sections and Raman depolarization ratios were calculated and these data are listed in Tables 2 and 3.

The PED (potential energy distribution) was constructed from a set of valence coordinates which are given in Table 4, referring to the numbers in Fig. 1. Only PED terms larger than 10% have been included in Tables 2 and 3 and the largest term in PED is also described in terms of valence coordinates in these tables. The C–H, C–Cl and Si–Cl stretching modes are reasonably well localized, but the CH_3 rock, C–C stretches and the skeletal deformations are highly mixed. Obviously, the vibrational modes for the *anti* conformer, separated into symmetry species a' and a'' are more localized than those of the *gauche* conformer in which all the modes belong to the same species.

DISCUSSION

Conformations

Neither the infrared vapour contours, the Raman depolarization data nor the *ab initio*-calculated energies can answer the question of whether the infrared and Raman bands present in the crystal belong to the *anti* or the *gauche* conformer. The infrared vapour contours can easily be mistaken for neighbouring conformer bands. The Raman spectra of the liquid frequently consisted of overlapping rotamer bands, making the depolarization ratios of limited value, and the energies for the *anti* and *gauche* conformers derived from the *ab initio* calculations have large uncertainties. However, the force constants and the wavenumbers obtained from the *ab initio* calculations after appropriate scaling usually give good agreement with those of the observed fundamentals. The shifts between the calculated wavenumbers of the *anti* and *gauche* conformers obtained after scaling are essential for determining which conformer is present in the crystal. Particularly when these shifts are large (>10 cm^{-1}) a comparison with the actual infrared and Raman spectra clearly identifies the conformers.

As is apparent from Tables 2 and 3, the calculated wavenumbers for the same mode of the *anti* and *gauche* conformers were separated by 10 cm^{-1} or more in six cases: ν_1, ν_{17}, ν_{18}, ν_{19}, ν_{20} and ν_{25}. In five of these instances, neglecting the CH stretching mode ν_1, the bands were assigned to conformational pairs in which the *gauche* conformer vanished and the *anti* conformer remained in the crystal. Also, when the shifts were calculated to be <10 cm^{-1}, separate band pairs with a few wavenumbers separation were frequently observed in the spectra. With these attributions the five *anti–gauche* shifts were qualitatively all in the right direction and the size of the shifts was also mostly in good agreement with the calculations (Tables 1–3).

Especially convincing are the shifts of ν_{17} and ν_{18} calculated to be 14 and 22 cm^{-1}, respectively. The corresponding observed shifts were 16 and 21 cm^{-1} with *anti* having the higher wavenumber for ν_{17} and *gauche* for ν_{18}. The PED values in Tables 2 and 3 reveal that ν_{17} is predominantly ClSiCl symmetrical stretch for both conformers while ν_{18} is highly mixed. The *anti* conformer of ν_{18} has the largest contribution to the PED from ClCCl bend whereas *gauche* had the ClCCl symmetric stretch as the largest term. It seems certain that the *anti* conformer is present in the crystal, since the alternative

Table 2. Observed and calculated fundamental modes of the *anti* conformer of dichloromethylmethyldichlorosilane (DCMDCS)

Obs.[a]			Calc.[b,c]							
$\tilde{\nu}$/cm^{-1}	I_{IR}	I_R	$\tilde{\nu}$/cm^{-1}	I_{IR}^{d}	I_R^{e}	ρ^{f}	ν		PED[g]	Approximate description
2965	w	m, P	2979	5	62	0.28	ν_1	a'	$100S_3$	CH stretch
2987	w	m, D	2931	2	62	0.75	ν_2	a''	$100S_{19}$	CH_3 antisym. stretch
2952	vw	m, P	2927	2	76	0.75	ν_3	a'	$74S_6 + 26S_7$	CH_3 antisym. stretch
2919	w	vs, P	2855	0	110	0.00	ν_4	a'	$100S_7$	CH_3 sym. stretch
1414	w	vw, P?	1408	6	8	0.75	ν_5	a''	$96S_{25}$	CH_3 antisym. deformation
1408	w	vvw	1407	5	5	0.74	ν_6	a'	$95S_{16}$	CH_3 antisym. deformation
1267	s	vw	1287	29	2	0.07	ν_7	a'	$95S_{14}$	$SiCH_3$ sym. deformation
1185[h]	w	w, P	1215	13	5	0.75	ν_8	a''	$97S_{20}$	$SiCH_3$ antisym. deformation
1143	m	w, P	1163	3	4	0.75	ν_9	a'	$89S_9$	C–H deformation
841	m	w, P	817	51	5	0.19	ν_{10}	a'	$28S_1 + 19S_4 + 30S_{15}$	Si–C(HCl_2) stretch
826	w	vw, D?	802	75	0	0.75	ν_{11}	a''	$85S_{24}$	$SiCH_3$ rock
797	vs	vw	782	48	4	0.53	ν_{12}	a'	$18S_1 + 13S_4 + 47S_{15}$	$SiCH_3$ rock
741	s	w, P	728	92	16	0.75	ν_{13}	a''	$85S_{17}$	CCl_2 antisym. stretch
728	m	m, D	706	50	6	0.74	ν_{14}	a'	$61S_2 + 16S_4$	Si–C(H_3) stretch
616[h]	m	s, P	585	57	9	0.01	ν_{15}	a'	$27S_1 + 30S_4 + 12S_{10}$	CCl_2 sym. stretch
580	vs	vw, D	538	161	4	0.75	ν_{16}	a''	$82S_{18} + 11S_{22}$	$SiCl_2$ antisym. stretch
494	m	vs, P	467	81	10	0.03	ν_{17}	a'	$67S_5 + 10S_{10}$	$SiCl_2$ sym. stretch
325	w	vs, P	353	3	9	0.27	ν_{18}	a'	$24S_4 + 12S_8 + 35S_{11}$	Cl–C–Cl bend
261	m	w, D?	286	19	1	0.67	ν_{19}	a'	$11S_8 + 21S_{10} + 28S_{11} + 19S_{13}$	$SiCCl_2$ sym. bend
239	vw	m, P?	256	2	3	0.75	ν_{20}	a''	$26S_{21} + 57S_{22}$	$SiCl_2$ rock
204	w	m, P	219	14	2	0.67	ν_{21}	a'	$35S_{12} + 53S_{13}$	$SiCl_2$ wag
194	vw	s, P?	191	0	2	0.75	ν_{22}	a''	$20S_{21} + 18S_{22} + 51S_{23}$	$SiCl_2$ twist
172	vw	s, P	177	1	2	0.69	ν_{23}	a'	$27S_{10} + 12S_{11} + 38S_{12}$	Cl–Si–Cl bend
155[i]		w	161	0	0	0.75	ν_{24}	a''	$97S_{27}$	CH_3 torsion
148	w	w, D	144	5	1	0.75	ν_{25}	a'	$61S_8 + 20S_{10} + 10S_{12}$	$SiCCl_2$ antisym. bend
114	w	w, P	110	1	0	0.75	ν_{26}	a'	$39S_{21} + 13S_{22} + 44S_{23}$	C–Si–C bend
62[i]		vw	47	1	0	0.75	ν_{27}	a''	$13S_{21} + 74S_{26}$	CH_2Cl torsion

[a] From infrared vapour spectra, except where noted.

[b] Calculated at the RHF/6–311G* level.

[c] Wavenumbers above 400 cm^{-1} have been scaled by 0.9; a' and a'' denote symmetry species.

[d] Calculated infrared intensities (km mol^{-1}).

[e] Calculated Raman cross-sections (Å^4 mol^{-1}).

[f] Depolarization ratios.

[g] For definition of symmetry coordinates, see Table 5; PED terms below 10% are omitted.

[h] IR spectra in argon matrix.

[i] Raman spectra of the liquid.

Table 3. Observed and calculated fundamentals of the *gauche* conformer in dichloromethyl methyl dichlorosilane (DCMDCS)

Obs.[a]			Calc.[b,c]						
$\tilde{\nu}$/cm^{-1}	I_{IR}	I_R	$\tilde{\nu}$/cm^{-1}	I_{IR}^{d}	I_R^{e}	ρ^{f}	ν	PED[g]	Approx. description
2965	w	m, P	2962	6	66	0.29	ν_1	$100S_3$	CH stretch
2987	w	m, D	2933	2	70	0.75	ν_2	$43S_6 + 19S_7 + 38S_{19}$	CH_3 antisym. stretch
2952	vw	m, P	2919	4	82	0.73	ν_3	$58S_6 + 15S_7 + 28S_{19}$	CH_3 antisym. stretch
2919	w	vs, P	2852	1	120	0.01	ν_4	$99S_7$	CH_3 sym. stretch
1414	w	vw, P	1410	6	8	0.75	ν_5	$12S_{16} + 84S_{25}$	CH_3 antisym. deformation
1408	w	vvw	1406	5	6	0.74	ν_6	$83S_{16} + 12S_{25}$	CH_3 antisym. deformation
1270	m	vw, P	1288	27	3	0.07	ν_7	$95S_{14}$	$SiCH_3$ sym. deformation
1191	w		1219	14	5	0.75	ν_8	$96S_{20}$	$SiCH_3$ antisym. deformation
1143	m	w, P	1165	1	5	0.71	ν_9	$89S_9$	C–H deformation
848	w		826	66	4	0.34	ν_{10}	$31S_1 + 18S_4 + 27S_{15}$	Si–C(HCl_2) stretch
826	w	vw, D?	802	78	0	0.75	ν_{11}	$12S_{15} + 73S_{24}$	$SiCH_3$ rock
791	m	m, P	782	27	7	0.45	ν_{12}	$10S_1 + 20S_4 + 31S_{15} + 13S_{17}$	$SiCH_3$ rock
745	s		729	104	14	0.65	ν_{13}	$74S_{17}$	CCl_2 antisym, stretch
732	s		703	58	6	0.49	ν_{14}	$78S_2$	Si–C(H_3) stretch
615	m	s, P	587	57	5	0.10	ν_{15}	$19S_1 + 22S_4 + 15S_{10} + 14S_{18}$	CCl_2 sym stretch
575	vs		533	158	3	0.66	ν_{16}	$71S_{18}$	$SiCl_2$ antisym. stretch
478	m	s, P	453	52	11	0.04	ν_{17}	$74S_5 + 10S_{10}$	$SiCl_2$ sym. stretch
346	w	vs, P	375	20	10	0.28	ν_{18}	$10S_1 + 25S_4 + 13S_{10} + 16S_{11} + 20S_{13}$	CCl_2 sym. stretch
266	w	w, P	298	19	2	0.64	ν_{19}	$15S_{10} + 43S_{11} + 29S_{13}$	Cl–C–Cl bend
248	vw	m, P	269	6	3	0.72	ν_{20}	$28S_8 + 18S_{12} + 20S_{21}$	C–Si–C bend
204	w	m, P	217	5	1	0.75	ν_{21}	$47S_{22} + 18S_{23} + 12S_{24}$	$SiCl_2$ rock
194	w	s, P?	197	0	2	0.64	ν_{22}	$18S_8 + 11S_{10} + 10S_{11} + 18S_{13} + 11S_{23} + 16S_{27}$	Skeletal deformation
172	vw	s, P?	180	2	3	0.72	ν_{23}	$52S_{12} + 16S_{21}$	Cl–Si–Cl bend
165[i]		m	169	0	0	0.68	ν_{24}	$71S_{27}$	CH_3 torsion
122[i]	w	w	120	1	1	0.70	ν_{25}	$32S_8 + 14S_{10} + 13S_{13} + 25S_{21}$	$SiCCl_2$ antisym. bend
115[i]		vw, D	114	2	1	0.75	ν_{26}	$15S_{10} + 18S_{21} + 14S_{22} + 49S_{23}$	$SiCl_2$ twist
62[i]	w	vw	46	0	1	0.75	ν_{27}	$88S_{26}$	CH_2Cl torsion

[a] From infrared vapour spectra, except where noted.
[b] Calculated at the RHF/6–311G* level.
[c] Wavenumbers above 400 cm^{-1} have been scaled by 0.9.
[d] Calculated infrared intensities (km mol^{-1}).
[e] Calculated Raman cross-sections (Å^4 mol^{-1}).
[f] Depolarization ratios.
[g] For definition of symmetry coordinates, see Table 5; PED terms below 10% are omitted.
[h] IR spectra in argon matrix.
[i] Raman spectra of the liquid.

Table 4. Symmetry coordinates for dichloromethylmethyldichlorosilane (DCMDCS)[a]

a'	$S_1 = \Delta R_{1,2}$
	$S_2 = \Delta R_{2,3}$
	$S_3 = \Delta R_{1,9}$
	$S_4 = (\Delta R_{1,10} + \Delta R_{1,11})/\sqrt{2}$
	$S_5 = (\Delta R_{2,7} + \Delta R_{2,8})/\sqrt{2}$
	$S_6 = (2\Delta R_{3,4} - \Delta R_{3,5} - \Delta R_{3,6})/\sqrt{6}$
	$S_7 = (\Delta R_{3,5} + \Delta R_{3,6})/\sqrt{2}$
	$S_8 = \Delta\alpha_{1,2,3}$
	$S_9 = (\Delta\alpha_{2,1,9} - \Delta\alpha_{10,1,9} - \Delta\alpha_{11,1,9})/\sqrt{3}$
	$S_{10} = (\Delta\alpha_{2,1,10} + \Delta\alpha_{2,1,11})/\sqrt{2}$
	$S_{11} = \Delta\alpha_{10,1,11}$
	$S_{12} = \Delta\alpha_{7,2,8}$
	$S_{13} = (\Delta\alpha_{1,2,7} + \Delta\alpha_{1,2,8} - \Delta\alpha_{3,2,7} - \Delta\alpha_{3,2,8})/\sqrt{2}$
	$S_{14} = (\Delta\alpha_{2,3,4} + \Delta\alpha_{2,3,5} + \Delta\alpha_{2,3,6} - \Delta\alpha_{5,3,6} - \Delta\alpha_{4,3,6} - \Delta\alpha_{4,3,5})/\sqrt{6}$
	$S_{15} = (2\Delta\alpha_{2,3,4} - \Delta\alpha_{2,3,5} - \Delta\alpha_{2,3,6})/\sqrt{6}$
	$S_{16} = (2\Delta\alpha_{5,3,6} - \Delta\alpha_{4,3,6} - \Delta\alpha_{4,3,5})/\sqrt{6}$
a''	$S_{17} = (\Delta R_{1,10} - \Delta R_{1,11})/\sqrt{2}$
	$S_{18} = (\Delta R_{2,7} - \Delta R_{2,8})/\sqrt{2}$
	$S_{19} = (\Delta R_{3,5} - \Delta R_{3,6})/\sqrt{2}$
	$S_{20} = (\Delta\alpha_{10,1,9} - \Delta\alpha_{11,1,9})/\sqrt{2}$
	$S_{21} = (\Delta\alpha_{2,1,10} - \Delta\alpha_{2,1,11})/\sqrt{2}$
	$S_{22} = (\Delta\alpha_{1,2,7} - \Delta\alpha_{1,2,8} + \Delta\alpha_{3,2,7} - \Delta\alpha_{3,2,8})/2$
	$S_{23} = (\Delta\alpha_{1,2,7} - \Delta\alpha_{1,2,8} - \Delta\alpha_{3,2,7} + \Delta\alpha_{3,2,8})/2$
	$S_{24} = (\Delta\alpha_{2,3,5} - \Delta\alpha_{2,3,6})/\sqrt{2}$
	$S_{25} = (\Delta\alpha_{4,3,6} - \Delta\alpha_{4,3,5})/\sqrt{2}$
	$S_{26} = (\Delta\tau_{9,1,2,3} - \Delta\tau_{11,1,2,7} - \Delta\tau_{10,1,2,8})/\sqrt{3}$
	$S_{27} = (\Delta\tau_{1,2,3,4} - \Delta\tau_{7,2,3,5} - \Delta\tau_{8,2,3,6})/\sqrt{3}$

[a] For numbering of atoms, see Fig. 1.

interpretation would be completely unacceptable from the calculations.

As mentioned above, some of the infrared bands of DCMDCS observed in the argon and nitrogen matrices are reduced or enhanced in intensity after annealing, interpreted as a displacement of the *anti* and *gauche* equilibrium. The concentrations of the conformers in the unannealed matrices at 5 K should correspond roughly to the equilibrium in the vapour phase at room temperature. After annealing, the high-energy conformer may pass the barrier and convert towards equilibrium, leading to distinct intensity changes. However, if the enthalpy difference between the conformers is very small in the matrices, the conformational equilibrium at the annealing temperatures may not be very different from that of the unannealed matrices. In that case only small variations in band intensities might be expected.

The changes are seen in Figs 8 and 9 and in Table 1, where various bands from the matrix spectra in argon, nitrogen and krypton are enhanced (arrows pointing upwards in Table 1) and others are reduced in intensity (arrows pointing downwards). Thus, in the argon matrices the doublet at 798 and 792 cm^{-1} (ν_{12} *anti*), the band at 742 cm^{-1} (ν_{13} *anti*) and the doublet at 723 and 722 cm^{-1} (ν_{14} *anti*) are all enhanced after annealing. The doublet at 1194 and 1189 cm^{-1} (ν_8 *gauche*) and the bands at 837 cm^{-1} (ν_{10} *gauche*) and 728 cm^{-1} (ν_{14} *gauche*) diminish slightly after annealing. In the nitrogen matrices the doublet at 799 and 792 cm^{-1} (ν_{12} *anti*), the band at 743 cm^{-1} (ν_{13} *anti*) the doublet at 731 and 729 cm^{-1} (ν_{14} *gauche*) and the doublet at 724 and 721 cm^{-1} (ν_{14} *anti*) were enhanced after annealing.

In the krypton matrices a doublet appeared at 1271 and 1269 cm^{-1} in the unannealed spectra; the high-wavenumber band was reduced after annealing and, the latter increased (Fig. 9). For reasons not understood these bands are absent in the argon and nitrogen matrix spectra both before and after annealing, although they have high intensity in the IR spectrum of the amorphous phase. They are assigned to ν_7 *gauche*, since they vanish in the crystal spectra, both IR and in Raman. The band at 1261 cm^{-1}, increasing in intensity after annealing, was found in all the matrix spectra and attributed to ν_7 *anti*. Additional bands which increased in intensity after annealing were 1187 cm^{-1} (ν_8 *anti*), 834 cm^{-1} (ν_{10} *anti*), 742 cm^{-1} (ν_{13} *anti*) and the doublets 723/722 cm^{-1} (ν_{14} *anti*), 573/570 cm^{-1} (ν_{16} *anti*) and 494/492 cm^{-1} (ν_{17} *anti*). In some cases bands which were attributed to the *gauche* conformer increased in intensity: 788/785 cm^{-1} (ν_{12} *gauche*) in argon but not in nitrogen and krypton, whereas the pair at 731/729 cm^{-1} (ν_{14} *gauche*) increased in nitrogen but diminished in argon matrices. Therefore, the annealing experiments in the three matrices suggest that *anti* is the low-energy conformer, but the results are not conclusive. It should be emphasized that all these intensity changes were small.

Small intensity changes after annealing were also observed for the related silanes bromomethyldimethylfluorosilane,[20] chloromethyldimethylfluorosilane,[21] chloromethyldimethylchlorosilane,[22] bromomethyldimethylchlorosilane,[23] dichloromethylmethyldifluorosilane,[24] bromomethyldimethylsilane,[25] chloromethylmethyldifluorosilane[26] and 2-chloroethyltrifluorosilane.[27] When the enthalpy difference between the conformers is lower than ca 0.4 kJ mol^{-1}, a conformational equilibrium will be established even at the low temperatures of the matrices (4–50 K), provided that the barrier is not unusually high, and no significant intensity changes will occur in the matrix spectra after annealing.

The bond moments of the C—Cl and Si—Cl bonds in DCMDCS are much larger than those of the other bonds in the molecule. Therefore, as derived from the *ab initio* calculations, the *gauche* conformer where a pair of the C—Cl and Si—Cl bonds is oriented *gauche* to each other (Fig. 1) should have a much larger dipole moment (3.19 D) than the *anti* rotamer (1.23 D). In several conformational systems a stabilization of the polar conformer in the liquid compared with the vapour and in polar compared with non-polar solvents has been reported,[30] in agreement with the dielectric theory first proposed by Onsager.[31] Since the enthalpy difference in the

matrices is expected to be similar to that of the vapour, we would expect a larger enthalpy difference in the matrices than that derived for the liquid (0.4 kJ mol^{-1}). This prediction is not supported by the matrix spectra, which suggest a low enthalpy difference between the conformers in all three matrices.

Phase transitions

During the extensive annealing experiments which were carried out in the infrared and Raman cryostats, various intensity changes were observed. As described above, the vapour was shock frozen on the window at 80 K forming a genuine amorphous solid. The spectra had broad features similar to those of the liquid, and no lattice bands were observed in the low-wavenumber region below 200 cm^{-1}. When the sample was annealed to temperatures of 120 and 129 K and recooled to 80 K, only small changes appeared and the sample was apparently still amorphous. Further annealing to 135 K, however, caused significant changes since the bands became sharper, many were shifted from the previous position, certain bands were split into doublets and lattice modes appeared in the low-wavenumber region. However, no bands vanished in this crystal.

Upon further annealing to 150 K the bands at 1264 and 1192 cm^{-1} vanished completely and those at 756, 565, 349, 346, 272 and 246 cm^{-1} vanished in part. These features are not easily explained. Apparently, the crystal formed at ca 135 K contained both conformers, while the crystal formed after annealing to 150 K had only the *anti* conformer in the crystal lattice. If the sample was annealed to still higher temperatures of 165, 180 and 210 K the spectra changed appearance and the bands were similar to the amorphous phase. Both conformers were now present in the sample and the lattice modes were no longer there. It is possible that the sample had melted in this temperature range, but this is contradicted by the fact that it remained on the vertical window. Another possibility is a transition to a plastic phase in which both conformers are present.

In three halogenated silanes dichloromethyldifluoromethylsilane,[24] bromomethyldimethylsilane and the Si deuterated analogue[25] and chloromethylmethyldifluorosilane[26] two different crystals were found. They were obtained by selective annealing of an amorphous solid, formed by depositing the vapour on a cold window (or cold finger) at 80 K. In all three compounds one of the two crystals appeared to be stable whereas the other was metastable, but each crystal contained a different conformer. Thus, it was possible to record spectral results for each conformer separately in these crystalline phases in both the infrared and Raman spectra. Very complete experimental results for each separate conformer were achieved for these molecules[24–26] allowing the rotamer bands to be assigned with high certainty. The formation of two crystals, each having a different conformer, is rare, but occurs sometimes when the energy difference between the conformers is low and the enthalpies of crystallization are favourable. In 2-chloroethyltrifluorosilane[27] studied recently, a similar situation to that in DCMDCS occurred. An intermediate crystal was formed after annealing, containing both conformers, while annealing to a higher temperature led to a crystal containing only one conformer.

Spectral assignments

The assignments to the *anti* and *gauche* conformers of the infrared and Raman spectra appear in Tables 1–3. The fundamentals of the *anti* and *gauche* conformers have both been numbered consecutively to make a comparison more convenient, rather than the conventional method in which the a' modes are listed before those of a'' in the *anti* conformer of symmetry C_s.

The fundamentals of the *anti* conformer divide themselves between 16 a' and 11 a'' of which the former are polarized and the latter depolarized in the Raman spectra. As is apparent from Table 2, the modes ν_3, ν_9 and ν_{25}, although belonging to species a', all have depolarization ratios very close to the depolarized value, shortened to 0.75 with two digits. The *gauche* fundamentals should all give rise to polarized bands. Therefore, the overlapping *anti* and *gauche* fundamentals might as a result give polarized Raman bands. With some exceptions the assigned a' fundamentals have polarized and the a'' depolarized Raman bands. Exceptions are the *anti* fundamentals ν_8, ν_{13} and ν_{20} which belong to species a'', but they have apparently polarized Raman bands. On the other hand, the *anti* modes ν_{14} and ν_{19} belong to species a' but the Raman bands appear depolarized. However, the calculated depolarization ratios 0.74 and 0.67 are both close to the depolarized value (Table 2). The infrared and Raman intensities predicted from the *ab initio* calculations also provide valuable help for the assignments.

The PED values in Tables 2 and 3 reveal that in both conformers 11 modes are well localized and 16 delocalized. As is apparent from the assignments listed in Tables 1–3, there are 12 fundamentals where the *anti* and *gauche* bands presumably overlap and 15 cases where they are separated. Among the latter there are several cases in which IR and/or Raman bands vanish in the crystal. However, in some instances (ν_8, ν_{10}, ν_{13}, ν_{14} and ν_{15}) the assignments of the *anti/gauche* conformers are based merely upon the observation of two separate sets of infrared bands in the vapour and in matrix spectra. In the Raman spectra of all these fundamentals only one band was observed both in the liquid and in the annealed and crystalline states. Therefore, the assignment of these six modes to separate *anti* and *gauche* pairs is fairly uncertain. The bands discussed below refer to the infrared vapour phase, except when specific bands in other phases are emphasized.

We expect four C–H stretching fundamentals ν_1–ν_4 with one hydrogen attached to the CCl_2 moiety and three to the methyl group of each conformer. Although the calculations suggest that the C–H stretches of the two conformers are

separated from 2 to 17 cm^{-1}, the spectra suggest overlapping bands for the *anti* and *gauche* conformers of all these fundamentals. Since the Raman band at 2989 cm^{-1} appears depolarized it is assigned to the CH_3 antisymmetric stretch ν_2 of species *a″* in the *anti* conformer. Generally, the calculated wavenumbers were too high in this range, suggesting that 0.9 is too high a scaling factor for this region. The CH stretch ν_1 is attributed to the bands around 2965 cm^{-1} whereas ν_3 is assigned to the IR and Raman bands around 2952 cm^{-1}. The CH_3 symmetric stretch ν_4 was predicted around 2850 cm^{-1} for both conformers and has the highest Raman intensity in the calculated spectrum (Tables 2 and 3). This fundamental was assigned to the Raman bands around 2916 cm^{-1} in the liquid, which are very intense. The very weak bands around 2850 cm^{-1} are considered to be overtones or combination bands.

In the range below 1500 cm^{-1} we expect the different modes connected with CH_3 deformation, CH bending and $SiCH_3$ rock. As is apparent from the results in Tables 2 and 3, these modes are fairly independent of the conformations since the calculated wavenumbers are nearly identical for both conformers. The two antisymmetric CH_3 deformations ν_5 and ν_6 are assigned to the infrared vapour bands at 1414 and 1408 cm^{-1} common to both the *anti* and *gauche* conformers, in excellent agreement with the calculated wavenumbers. The CH_3 deformation ν_7 appears as closely spaced *gauche* and *anti* modes at 1270 and 1267 cm^{-1}, respectively, where the *gauche* component vanished in the crystal spectra. These IR bands are more intense than the neighbouring fundamentals, in agreement with the calculations (Tables 2 and 3). The CH_3 deformation ν_8 appeared at 1191 cm^{-1}, but had separate *gauche* and *anti* components in the matrix spectra. The CH deformation ν_9 with overlapping conformer bands was attributed to the vapour band with rotational fine structure at 1146 and 1141 cm^{-1}.

Both from the spectra (Table 1) and the calculations (Tables 2 and 3) it was evident that no fundamentals of DCMDCS were present in the spectral range from 1140 to 850 cm^{-1}. The mode ν_{10} has approximately equal contributions from Si–C(H_2Cl) stretch and $SiCH_3$ rock and involving also C–Cl stretch for both conformers. It appeared at 848 cm^{-1} (*gauche*) and 841 cm^{-1} (*anti*) in the vapour and in the matrices, but seemingly overlapped at ca 838 cm^{-1} in the condensed phases. The two modes $\nu_{11}(a'')$ and $\nu_{12}(a')$ involve predominantly out-of-plane and in-plane $SiCH_3$ rock and are both predicted to have completely overlapping rotamer bands at 802 and 782 cm^{-1}, respectively. The ν_{11} mode is assigned to the vapour band at 826 cm^{-1} common to both rotamers, whereas ν_{12} appeared as separate peaks both in the IR and Raman spectra, situated as a doublet at 798/796 (*anti*) and as a band at 791 cm^{-1} (*gauche*).

The fundamentals ν_{13}–ν_{18} between 750 and 350 cm^{-1} involve predominantly stretching vibrations between the heavy skeleton atoms C, Si and Cl. The CCl_2 antisymmetric stretch ν_{13} of species *a″* is attributed to the near-lying IR bands in the vapour and matrices at 745 (*gauche*) and 741 cm^{-1} (*anti*). They overlapped in the Raman spectra and therefore the polarized band at 741 cm^{-1} may be assigned to the *a″* fundamental for the *anti* rotamer (polarization ratio 0.75) coinciding with the *gauche* mode (polarization ratio 0.65). The Si$C(H_3)$ stretch ν_{14} was attributed to the vapour bands at 732 (*gauche*) and 728 cm^{-1} (*anti*), but they overlapped in the Raman spectra of the liquid, amorphous solid and crystal. The calculated polarization ratios for the *anti* and *gauche* modes were 0.74 and 0.49, respectively, and the 721 cm^{-1} band was observed as a depolarized Raman band. The 745/741 cm^{-1} bands might instead be attributed to ν_{14} and the 732/728 cm^{-1} bands to ν_{13}, in better agreement with the depolarization measurements, but this alternative is not supported by the calculated wavenumbers.

According to the PED, the mode ν_{15} is highly mixed between various symmetry coordinates, but the symmetric CCl_2 stretch gives the largest contribution. Tentatively, the *anti* and *gauche* components are attributed to neighbouring IR bands in the matrices and the solids, but in the vapour and in the Raman spectra only one band was detected. The two modes ν_{16} at 580 (*anti*) and 575 cm^{-1} (*gauche*) and ν_{17} at 494 (*anti*) and 478 cm^{-1} (*gauche*) involve $SiCl_2$ antisymmetric and symmetric stretch, respectively. These modes are separated by 5 and 16 cm^{-1} into *anti* and *gauche* components with shifts in excellent agreement with the calculations; the former is very strong in the IR and the latter in the Raman spectra, as predicted.

The fundamentals involving deformations of the heavy atoms are expected below 350 cm^{-1} and some of these are predicted to have large shifts between the *anti* and *gauche* components. Many of these modes are mixed between various symmetry coordinates, particularly for the *gauche* conformer, and the 'approximate description' in terms of valence coordinates is ambiguous. Also, the largest PED contribution in the *anti* conformer was frequently different from that of the *gauche* conformer. No infrared matrix spectra were recorded in this region, making the experimental data less conclusive. The ν_{18} mode was observed at 325 for the *anti* and at 346 cm^{-1} for the *gauche* conformer. The observed shift of 21 cm^{-1} is in excellent agreement with the calculated value of 22 cm^{-1}, but the doublet at 348/344 cm^{-1} was still present in the crystal spectra in the infrared. The ν_{19} mode was tentatively attributed to the bands at 266 (*gauche*) and 261 cm^{-1} (*anti*), with a smaller shift (5 cm^{-1}) than the calculated value of 12 cm^{-1}. Both the infrared and the Raman band of the assumed *gauche* component were merely reduced in intensity in the crystal spectra.

The ν_{20} modes were assigned to the vapour bands at 248 (*gauche*) and 239 cm^{-1} (*anti*) while the ν_{21} modes coincided at 204 cm^{-1}. The *anti* mode of ν_{20} and the *gauche* mode of ν_{21} involved predominantly $SiCl_2$ rock, but these deformation modes are highly delocalized. Both the ν_{22} and ν_{23} modes were assigned to overlapping rotamers with vapour bands at

194 and 172 cm^{-1}, respectively, although the two unassigned Raman bands at 185 cm^{-1} might be due to a second conformer of ν_{22}. The CH_3 torsion (ν_{24}) should be very weak in the IR and Raman spectra according to the calculations. The weak Raman bands at 165 and 155 cm^{-1} with no infrared counterparts were attributed to these *gauche* and *anti* modes, respectively. The deformation mode $\nu_{25}(a')$ was attributed to infrared bands of the amorphous spectra at 148 (*anti*) and 140 cm^{-1} (*gauche*), both with Raman counterparts. The mixed bending mode $\nu_{26}(a'')$ was found at 114 (*gauche*) and 111 cm^{-1} (*anti*), respectively. Finally, the CH_2Cl torsion was tentatively assigned to the Raman band at 62 cm^{-1} in the liquid and at slightly higher values in the IR and Raman spectra in the low-temperature phases. The three Raman bands at 47, 37 and 31 cm^{-1} observed in the crystal spectra are probably due to lattice modes.

Acknowledgements

Very helpful assistance from Anne Horn, Oslo, is gratefully acknowledged. V. Aleksa received a scholarship granted to the Baltic Countries and Northwest Russia from the Norwegian Research Council and A. Gruodis was supported by the Norwegian Academy of Science and Letters.

REFERENCES

1. Gruodis A, Powell DL, Klaeboe P, Nielsen CJ, Aleksa V, Guirgis GA, Durig RJ. *J. Mol. Struct.* 2001; in press.
2. Qtaitat MA, Durig JR. *Spectrochim. Acta, Part A* 1993; **49**: 2139.
3. Afifi MS, Guirgis GA, Mohamed TA, Herrebout WA, Durig JR. *J. Raman Spectrosc.* 1994; **25**: 159.
4. Durig JR, Guirgis GA, Mohamed TA, Herrebout WA, Afifi MS. *J. Mol. Struct.* 1994; **319**: 109.
5. Durig JR, Sullivan JF, Guirgis GA, Qtaitat MA. *J. Phys. Chem.* 1991; **95**: 1563.
6. Durig JR, Guirgis GA, Qtaitat MA. *J. Raman Spectrosc.* 1995; **26**: 413.
7. Durig JR, Guirgis GA, Kim YH, Yan W, Qtaitat MA. *J. Mol. Struct.* 1996; **382**: 111.
8. Hassler K, Köll W, Schenzel K. *J. Mol. Struct.* 1995; **348**: 353.
9. Ernst M, Schenzel K, Jähn A, Hassler K. *J. Mol. Struct.* 1997; **412**: 83.
10. Ernst M, Schenzel K, Jähn A, Köll W, Hassler K. *J. Raman Spectrosc.* 1997; **28**: 589.
11. Zink R, Hassler K, Ramek M. *Vib. Spectrosc.* 1998; **18**: 123.
12. Johansen T, Hagen K, Hassler K, Tekautz G, Stølevik R. *J. Mol. Struct.* 1999; **237**: 509.
13. Jähn A, Schenzel K, Zink R, Hassler K. *Spectrochim. Acta, Part A* 1999; **55**: 2677.
14. Schenzel K, Hassler K. *Spectrochim. Acta, Part A* 1996; **52**: 637.
15. Jähn A, Schenzel K, Zink R, Hassler K. *J. Raman Spectrosc.* 1998; **29**: 841.
16. Jähn A, Schenzel K, Zink R, Hassler K. *J. Raman Spectrosc.* 1998; **29**: 1055.
17. Wojnowski W, Konieczny S, Dreczewski B, Herman B. *Przem. Chem.* 1989; **68**: 409.
18. Miller F, Harney BM. *Appl. Spectrosc.* 1970; **24**: 291.
19. Hallam HE. *Vibrational Spectroscopy of Trapped Species*. Wiley: London, 1973; 39.
20. Jensen HM, Klaeboe P, Aleksa V, Nielsen CJ, Guirgis GA. *Acta Chem. Scand.* 1998; **52**: 578.
21. Aleksa V, Klaeboe P, Nielsen CJ, Guirgis GA. *J. Mol. Struct.* 1998; **445**: 161.
22. Jensen HM, Guirgis GA, Klaeboe P, Nielsen CJ, Aleksa V. *Acta Chem. Scand.* 1998; **52**: 1359.
23. Nilsen A, Klaeboe P, Nielsen CJ, Guirgis GA, Aleksa V. *J. Mol. Struct.* 2000; **550–551**: 199.
24. Aleksa V, Klaeboe P, Horn A, Nielsen CJ, Guirgis GA. *J. Raman Spectrosc.* 1998; **29**: 627.
25. Aleksa V, Klaeboe P, Nielsen CJ, Tanevska V, Guirgis GA. *Vibr. Spectrosc.* 1998; **17**: 1.
26. Aleksa V, Klaeboe P, Nielsen CJ, Gruodis A, Guirgis GA, Herzog K, Salzer R, Durig JR. *J. Raman Spectrosc.* 2000; **31**: 897.
27. Klaeboe P, Nielsen CJ, Aleksa V, Gruodis A, Guirgis GA, Nashed YE, Durig RJ. *J. Mol. Struct.* in press.
28. Barnes AJ. *J. Mol. Struct.* 1984; **113**: 161.
29. Frisch MJ, Trucks GW, Schlegel HB, Gill MW, Johnson BG, Robb MA, Cheeseman JR, Keith T, Petersson GA, Montgomery JA, Raghavachari K, Al-Laham MA, Zakrzewski VG, Ortiz JV, Foresman JB, Cioslowski J, Stefanov BB, Nanayakkara A, Challacombe M, Peng CY, Ayala PY, Chen W, Wong MW, Andre JL, Replogle ES, Martin RL, Fox DJ, Binkley JS, Defrees DJ, Baker J, Stewart JP, Head-Gordon M, Gonzalez C, Pople JA. *Gaussian 94, Revision D.2*. Gaussian: Pittsburgh, PA, 1995.
30. Abraham RJ, Bretschneider E. In *Internal Rotation in Molecules*, Orville-Thomas WJ (ed). Wiley: London, 1974; 481.
31. Onsager L. *J. Am. Chem. Soc.* 1936; **58**: 1.